Comparison of Experiment and Theory for Nuclear Excitation in ^{115}In by Threshold-Energy Electrons*

B. T. CHERTOK† AND W. T. K. JOHNSON†
The American University, Washington, D. C. 20016
(Received 13 May 1968)

The Duke inelastic-electron-scattering program provides a major step in obtaining spin-parity assignments and mixing ratios for nuclear energy levels from threshold-energy electron scattering which populates an isomer. A detailed account of the Duke distorted-wave Born-approximation calculation for threshold-energy electrons is given, and the contribution and Coulomb distortion of the partial waves for $M1$ and $E2$ transitions is quantitatively presented. The finite tip observed in threshold electroexcitation is quantitatively accounted for by Coulomb distortion of s- and d-electron waves in the $M1$ and $E2$ transitions, respectively. A detailed comparison is made between experiment and theory for the 1.078- and 1.450-MeV states of $_{49}{}^{115}\mathrm{In}_{66}$, replacing earlier semiquantitative comparisons which used plane-wave Born-approximation calculations that resulted in factors of 2–5 disagreement for 1–2-MeV electrons. The agreement between the electron excitation functions for isomer population for the 1.078- and 1.450-MeV states and the Duke calculation is well within the $\pm 35\%$ experimental errors. $M1/E2$ mixing ratios are extracted from the comparison. The 1.078- and 1.450-MeV states of ^{115}In are both $\frac{7}{2}^+$ with $M1/E2$ mixing ratios, $a=\Gamma_{0E2}/\Gamma_{0M1}$, given by $a=0.7\pm 0.3$ and ≤ 0.3, respectively. The mixing ratios are from photon self-absorption and Coulomb-excitation measurements of the same transitions, and corroborate the electron-scattering results. In this regard a search for the 1.078-MeV γ ray following β^- decay of ^{115m}Cd using a Ge(Li) Duode spectrometer yielded a null result, $\log ft>11.5$ for the β^- transition. With the $\frac{7}{2}^+$ assignments made in this work, the coexistence of spherical and rotational bands in ^{115}In is discussed.

1. INTRODUCTION

EXCITATION of energy levels of medium and heavy weight nuclei by threshold-energy electrons is at a stage of development comparable to studies of internal-conversion electrons before calculations of Rose *et al.*[1] which used the electron wave functions from the solution of the Dirac equation with the Coulomb potential. Plane-wave Born-approximation (PWBA) calculations of inelastic electron scattering[2–4] have existed for some years; however, multipolarity assignments and transition widths from electron-scattering experiments could be made only semiquantitatively because of the neglect of Coulomb distortion of the electron waves in the field of the nucleus. Attempts to patch up the PWBA theory for this effect via nuclear Coulomb functions $F(Z,p)/F(Z,p_0)$ indicated large effects of Coulomb distortion (factors of 2–5) where the larger corrections are closer to threshold.[5] Even with these corrections the inelastic electron cross sections were about 50% of the experimental value. Recently, Tuan, Wright, and Onley[6] extended their distorted-wave Born-approximation (DWBA) calculation, which uses a partial-wave analysis of the Dirac equation containing the Coulomb potential of the ground-state charge distribution, to solve the inelastic-electron-scattering problem down to threshold, $E_0>m_0c^2$. We present here a quantitative comparison of their calculation with our electron-excitation experiments on $_{49}{}^{115}$In which have been improved and extended by Booth and Brownson.[7] The calculation has evolved from the high-energy elastic-electron-scattering partial-wave analysis of Yennie, Ravenhall, and Wilson[8] which was reformulated in the DWBA to include nuclear excitation by Griffy, Onley, Reynolds, and Biedenharn.[9]

We make the comparison with the 1.078- and 1.450-MeV levels of ^{115}In to illustrate the role of our isomer activation measurements in studies of electromagnetic interactions in nuclei.

The energy spectrum of ^{115}In up to 1.5 MeV has been studied extensively with increasing convergence on spin and parity assignments, transition strengths, and intralevel transitions.[10–12] At the same time, nuclear model calculations have had very limited success which is somewhat surprising since the levels up to 600 keV, namely $0(\frac{9}{2}^+)$, $336(\frac{1}{2}^-)$, and $597(\frac{3}{2}^-)$, fit into the extreme single-particle coupling scheme; and the next higher levels, namely $829(\frac{3}{2}^+)$, $864(\frac{1}{2}^+, \frac{3}{2}^+)$, and $934(\frac{7}{2}^+)$, appear to indicate the base of a rotational band on the 864-keV state. The next five states 1078, 1133, 1291, 1419, and 1450 keV make fast $M1$ and/or $E2$ transitions to ground but only two are picked out in our isomer activation measurements.[5,7] The 1078- and 1450-keV

* Research supported by the National Science Foundation.
† Guest workers, National Bureau of Standards.
[1] M. Rose, G. Goertzel, B. Spinrad, J. Harr, and P. Strong, Phys. Rev. **83**, 79 (1951).
[2] K. Alder, A. Bohr, T. Huus, B. Mottleson, and A. Winther, Rev. Mod. Phys. **28**, 432 (1956).
[3] H. Robl, Nucl. Phys. **2**, 641 (1956).
[4] R. Willey, Nucl. Phys. **40**, 529 (1963).
[5] B. Chertok and E. Booth, Nucl. Phys. **66**, 230 (1965).
[6] S. Tuan, L. Wright, and D. Onley, Nucl. Instr. Methods **60**, 70 (1968).
[7] E. Booth and J. Brownson, Nucl. Phys. **A98**, 529 (1967).
[8] D. Yennie, D. Ravenhall, and R. Wilson, Phys. Rev. **95**, 500 (1954).
[9] T. Griffy, D. Onley, J. Reynolds, and L. Biedenharn, Phys. Rev. **128**, 833 (1962).
[10] G. Graeffe, C. Tang, C. Coryell, and G. Gordon, Phys. Rev. **149**, 884 (1966).
[11] A. Bäcklin, B. Fogelburg, and S. Malmskog, Nucl. Phys. **A96**, 539 (1967).
[12] J. McDonald, D. Porter, and D. Stewart, Nucl. Phys. **A104**, 177 (1967).

energy levels are known[10,11] to cascade down to the 336-keV isomer via direct transitions to the 849- and 864-keV rotational levels. As noted in Fig. 1 and in Fig. 7, the isomer measurement selects only those nuclear levels which are strongly connected to the ground state and have a finite branching ratio Γ_{iso}/Γ to a low-lying isomer level. In this way one measures electroexcitation in the absence of the intense bremsstrahlung background, i.e., between beam pulses or with the accelerator turned off. Since we measure the product $B(L,\uparrow)\times\Gamma_{iso}/\Gamma$, the levels may result from mixing of the spherical and rotational bands. We shall deduce the multipolarity and mixing ratios for the 1078- and 1450-keV transitions by fitting the DWBA electron-scattering cross section to our experimental excitation function and compare the results with those from measurements of the total radiative width and $B(E2,\uparrow)$ of the 1078- and 1450-keV levels.

In the sections that follow, we develop the equations for electron and photon excitation, describe the partial-wave analysis program with regard to methods, nuclear model independence, comparisons with PWBA cross sections, and comparisons of experiment with theory in ^{115}In. In Sec. 5, the status of ^{115}In up to 1.45-MeV excitation is discussed in light of the spin-parity assignments from electron scattering, photon self-absorption, and Coulomb-excitation experiments.[12] The results of our search for the 1.078-MeV γ ray following the β^- decay of ^{115m}Cd are reported.

2. THEORY

For electron scattering producing nuclear excitation of electric and magnetic multipolarities EL and ML, the total cross section is

$$\sigma_{e,e'}=\sum_{L=0}^{\infty}\sigma_{EL}+\sum_{L=1}^{\infty}\sigma_{ML}, \tag{1}$$

where the electric transitions can be subdivided into those produced by a virtual photon longitudinal (C) and transverse (T) to the direction of momentum transfer.[13]

$$\sum_{L=0}^{\infty}\sigma_{EL}=\sum_{L=0}^{\infty}\sigma_{CL}+\sum_{L=1}^{\infty}\sigma_{TL}. \tag{2}$$

At threshold energies $E\geq k$, both terms contribute[14] but it does not appear feasible to experimentally separate the σ_{CL} and σ_{TL} except for electric monopole transitions, although at much higher electron energies the separation is straightforward through measurement of the differential scattering cross section.

We give the explicit form of the differential cross section for magnetic transitions derived in the PWBA,[4]

$$\frac{d\sigma}{d\Omega}=\frac{4\pi\alpha^2}{[(2L+1)!!]^2}\frac{L+1}{L}\frac{q^{2L}}{p_0{}^2}B(ML,q,I_fI_i)V_T(\theta), \tag{3}$$

where $B(ML,q,I_fI_i)$ is the reduced nuclear transition probability for the upward transition and the other terms have their standard definitions except that we do not neglect m_0c^2 in $V_T(\theta)$ or the $V_L(\theta)$ in the electric transitions. p_0 is the momentum of the incident electron and the momentum transfer, $\mathbf{q}=\mathbf{p}_0-\mathbf{p}$.

The integration over angle yields a total cross section where we denote an average value of momentum transfer $\bar{q}$ for B since one measures all q from (p_0-p) to (p_0+p).[15]

$$\sigma_{ML}=G(L,E_0,k)B(ML,\bar{q},I_fI_i). \tag{4}$$

The cross section in the long-wavelength limit $q\rightarrow k$ becomes

$$\sigma_{e,e'}=F(L,E_0,k)g\Gamma_0/m_0c^2, \tag{5}$$

where the F's were first defined by Robl[3] in the PWBA for electric and magnetic transitions. Γ_0 is the radiative width of the excited-to-ground-state transition. One uses a detailed balance and a definition in going from Eq. (4) to Eq. (5), i.e.,

$$B(ML,q,I_fI_i)=gB(ML,q,I_iI_f)$$
$$\underset{q\rightarrow k}{=}\frac{g\Gamma_0}{\alpha\hbar c}\frac{L}{L+1}\frac{[(2L+1)!!]}{8\pi}\frac{1}{(k/\hbar c)^{2L+1}}. \tag{6}$$

We measure isomer activation by electron scattering as in Fig. 1, where

$$\sigma_{iso,e}=\sigma_{e,e'}\Gamma_{iso}/\Gamma. \tag{7}$$

For parity-favored transitions $\pi_i\pi_f=(-1)^{I_i-I_f}$,

$$\sigma_{iso,e}=\frac{g\Gamma_0\Gamma_{iso}}{m_0c^2\Gamma}\left[\frac{F_{EL}}{1+a}+\frac{F_{M(L+1)}}{1+a^{-1}}\right], \tag{8}$$

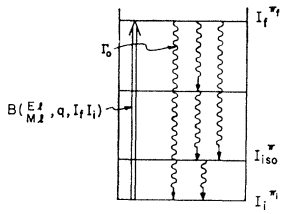

FIG. 1. A nuclear-energy-level diagram depicting a typical isomer activation scheme is presented, where the value of I_f is intermediate between I_i and I_{iso} and transitions of low multipolarity, $L=(0)$, 1 and 2 are most probable at threshold electron energies. The direct transition, $I_i\rightarrow I_{iso}$, is forbidden by the large $L\geq|I_{iso}-I_i|$ and small excitation energy, and the cascade to the isomer, from experience with ^{115}In, is more probable than the cross-over transition $I_f\rightarrow I_{iso}$.

[13] W. Barber, Ann. Rev. Nucl. Sci. **12**, 1 (1962).

[14] B. Chertok, Bull. Am. Phys. Soc. **11**, 338 (1966).

[15] There is some question over the q dependence in the definition of B. In any case for $q\rightarrow k$ one can go from (3) directly to (5) without ambiguity.

where the mixing ratio, $a=\Gamma_0(M(L+1))/\Gamma_0(EL)$ and $\Gamma_0=\Gamma_0(EL)+\Gamma_0(M(L+1))+\cdots$. For parity-unfavored transitions $\pi_i\pi_f=(-1)^{I_i-I_f+1}$,

$$\sigma_{\mathrm{iso},e}=\frac{g\Gamma_0\Gamma_{\mathrm{iso}}}{m_0c^2\Gamma}\left[\frac{F_{ML}}{1+a}+\frac{F_{E(L+1)}}{1+a^{-1}}\right], \tag{9}$$

where $a=\Gamma_0(E(L+1))/\Gamma_0(ML)$ and $\Gamma_0=\Gamma_0(ML)+\Gamma_0\times(E(L+1))+\cdots$. For the special case $I_i^\pi=I_f^\pi$,

$$\sigma_{\mathrm{iso},e}=\frac{g\Gamma_0\Gamma_{\mathrm{iso}}}{m_0c^2\Gamma}\left[\frac{F_{E0}\Gamma_e}{\Gamma_0-\Gamma_e}+\frac{F_{ML}}{1+a}+\frac{F_{E(L+1)}}{1+a^{-1}}\right], \tag{10}$$

where Γ_e includes internal-conversion and pair-creation widths. For completeness the monopole cross section is derived in the Appendix.

A photoexcitation measurement of the same transition (excluding the special $E0$ case) gives an integrated cross section $\int\sigma_{\mathrm{iso}}dE$ for populating an isomer through a higher level as in Fig. 1. Integration of the Bethe-Placzek photon-scattering cross section over an isolated nuclear level in the Doppler-broadened limit, i.e., $\Delta\gg\Gamma_0$, yields

$$\int\sigma_{\mathrm{iso}}dE\equiv\left[\int\sigma_\gamma dE\right]\frac{\Gamma_{\mathrm{iso}}}{\Gamma}=\tfrac{1}{4}\lambda^2\frac{g\Gamma_0\Gamma_{\mathrm{iso}}}{\Gamma}, \tag{11}$$

where λ is the wavelength of the resonance radiation and $g=(2I_f+1)/(2I_i+1)$ in the notation of Fig. 1.

The ratio of electron-to-photon excitation gives the meeting ground between experiment and theory,

$$F=\left(\sigma_{\mathrm{iso},e}\Big/\int\sigma_{\mathrm{iso}}dE\right)\tfrac{1}{4}\lambda^2m_0c^2, \tag{12}$$

where the F_{expt} is to be compared to the bracketed expressions in 8–10. We will extract F_{theor} from the DWBA calculation in Sec. 3. Note that the physics is analogous to the internal-conversion method where the electron-to-photon yield is measured and multipolarity of the transition is made from a comparison with a theoretical quantity, the internal-conversion coefficient, which is independent of the nuclear wave functions and transition operators.[16] A significant difference between our method and internal conversion is the measurement of an excitation function in the electroexcitation so that a unique mixing ratio must fit the slope.

Without any knowledge of I_f, one searches for a mixing ratio a, which gives a fit to the excitation function F_{expt} versus T_0, where T_0 is the incident kinetic energy of the electron. Determination of I_f is facilitated since the measurement connects the higher state with both the isomer and ground states as in Fig. 1, and low multipolarities are probable for nuclear excitations at threshold electron energies. A separate nuclear photon self-absorption or Coulomb-excitation measurement, together with the mixing ratio a, fixes the partial and total widths for the ground-state transition. When both $g\Gamma_0$ and $B(E2,\uparrow)$ are available (which is still the exception for odd-A nuclei near shell closures in the 0.5–3-MeV region), one has a check on the consistency through the independent measurement of the mixing ratio by electron excitation.

3. PARTIAL-WAVE ANALYSIS

A. Outline of Calculation

The Duke computer program[6,17] for inelastic electron scattering resulting from nuclear excitation was used to calculate the total cross sections for various possible multipolarities for the 1.078- and 1.450-MeV levels of $_{49}^{115}$In. This program uses a partial-wave analysis of the inelastic-electron-scattering problem where the electron plane waves are replaced by electron waves, distorted by the monopole part of the static Coulomb potential. This computer code, written in a recent version for higher-energy electrons, $E_0>30$ MeV, was modified to allow computation near threshold excitation energies. (As a check on the computational accuracy, the program could also calculate the PWBA.) By reducing the initial integration step and increasing the number of steps in the region within the nuclear surface, we are able to get convergence of the inelastic electron cross section down to electron energies 5 keV above threshold and numerical agreement within 1% for all multipolarities between the PWBA cross section using the Duke program and the direct computation of Robl,[3] Alder *et al.*,[2] etc. The Duke program was originally designed for electric transitions only; however, modification suggested by Tuan and Wright allowed us also to calculate magnetic transitions.

The following outline is based on a comprehensive discussion of the program and theory by Ziegler.[17] His notation is used throughout.

The theory assumes (1) single photon exchange, (2) that both ground and excited states have spherically symmetric charge distributions, (3) that nuclear recoil is negligible, (4) that incident electrons are unpolarized, and (5) that the detector will not differentiate between polarizations of the electrons.

The wave functions used are derived by a partial-wave expansion,

$$\psi_{\mathrm{tot}}{}^m=N\sum_{\kappa,\mu}e^{i\delta_\kappa}i^lY_l{}^{(\mu-m)*}(\hat{\rho})C_{\mu-m,m,\mu}{}^{l\frac{1}{2}j}\psi_\kappa{}^\mu,$$

where κ is the spin-angular momentum eigenvalue of $(\boldsymbol{\sigma}\cdot\mathbf{l}+1)$, C is the Clebsch-Gordan coefficient, μ is the eigenvalue of j_z, N is the normalization, δ_κ is the phase factor or phase shift for each k wave, m is the eigenvalue

[16] J. Hamilton, in *Nuclear-Spin Parity Assignments* (Academic Press Inc., New York, 1966).

[17] J. Ziegler, AEC Report No. TID-4500, Yale-2726E-49, 1967 (unpublished).

of $\sigma_z=\pm\frac{1}{2}$, $\hat{\rho}$ is the angle between the z axis and motion of the electron, are $\psi_\kappa{}^\mu$ are the eigenfunctions of the Dirac equation with central nuclear Coulomb potential

$$\psi_\kappa{}^\mu=\begin{bmatrix} g(r)\chi_\kappa{}^\mu \\ if(r)\chi_{-\kappa}{}^\mu \end{bmatrix}.$$

The interaction Hamiltonian which represents one-photon exchange is

$$H_{\rm int}=4\pi e^2\int\int[\rho_e G\rho_N-\mathbf{j}_e\cdot\mathbf{G}\cdot\mathbf{j}_N]d\tau_e d\tau_N,$$

where ρ_e and j_e (ρ_n and j_n) are the electron (nucleus) charge and current density operators where j_n includes nuclear magnetization. The G and $\mathbf{G}$ are the Green's function for the scalar and vector Helmholtz equations, where

$$\rho_e=(\psi_{\rm f}{}^\dagger\psi_{\rm i})_e=(f_k f_{k'}+g_k g_{k'})\ \text{(angular terms)},$$
$$\rho_N=\rho_1 Y_L{}^M,\quad j_e=\psi_{\rm f}{}^{(e)\dagger}\boldsymbol{\alpha}_e\psi_{\rm i}{}^{(e)},$$

and

$$\mathbf{j}_N=\rho_2\mathbf{Y}_{L,L-1}{}^M+\rho_3\mathbf{Y}_{L,L+1}{}^M+\rho_4\mathbf{Y}_{L,L}{}^M.$$

An example of one radial matrix element is the Coulomb radial integral of the interaction Hamiltonian,

$$R_{\rm Coul}=\frac{i}{K}\int\int[\rho_1(f_\kappa f_{\kappa'}+g_\kappa g_{\kappa'})j_l(Kr)h_l(Kr)]\times r_e{}^2 r_N{}^2 dr_e dr_N,$$
$$=\frac{1}{I}\int_0^\infty(f_\kappa f_{\kappa'}+g_\kappa g_{\kappa'})C_1 dx,$$

where

$$I\equiv\frac{(2L+1)!!}{\epsilon^L}\int j_L(\epsilon x)\rho_1(x)x^2dx,$$

$$x\equiv r(E_{\rm i}E_{\rm f}-m_0{}^2)^{1/2}/\hbar c,\quad \epsilon=(E_{\rm i}-E_{\rm f})/(E_{\rm i}E_{\rm f}-m_0{}^2)^{1/2},$$

and

$$Kr=\epsilon x.$$

$E_{\rm i}$ and $E_{\rm f}$ are the total electron energies and m_0 is the rest mass of the electron. C_1 is a cutoff function for the scalar interaction, L is the multipolarity of the transition, and l is the partial-wave number.

TABLE I. Model independence of Duke electron-scattering program.

c (F)	5.23[a]	5.23	5.76
t (F)	2.29	2.52	2.29
$\sigma(E2)/B(\uparrow)$, DWBA	2.13×10^{-4} [b]	2.13×10^{-4}	2.17×10^{-4}
$\sigma(E2)/B(\uparrow)$, PWBA	8.06×10^{-5}	7.96×10^{-5}	7.99×10^{-5}
$\sigma(M1)/B(\uparrow)$, DWBA	5.74×10^{-3}	5.70×10^{-3}	5.69×10^{-3}
$\sigma(M1)/B(\uparrow)$, PWBA	1.28×10^{-3}	1.28×10^{-3}	1.28×10^{-3}

[a] B. Hahn, D. Ravenhall, and R. Hofstadter, Phys. Rev. **101**, 1131 (1956).
[b] Calculations done for 1.078-MeV state of $_{49}{}^{115}$In with $T_0=1.30$ MeV.

By means of the incompressible irrotational-flow liquid-drop model, the transition charge and current distributions corresponding to *electric* multipole excitations are related to the ground-state charge distribution ρ_0 by

$$\rho_1=x^{L-1}\frac{d\rho_0}{dr},\quad \rho_2=x^{L-1}\left(\frac{2L+1}{L}\right)^{1/2}\rho_0,\quad \rho_3,\ \rho_4=0.$$

For the *magnetic* multipole excitations they are

$$\rho_1,\ \rho_2,\ \rho_3=0,\quad \rho_4=x^{L-1}(d\rho_0/dr),$$

where c is the nuclear half-density radius, t is the nuclear skin thickness, and $\rho_0=[1+\exp(r-c)/t]^{-1}$.

Briefly, the Duke program computes the inelastic-electron-scattering cross section by evaluating the interaction Hamiltonian matrix element $\langle H_{\rm int}\rangle_{\rm if}\simeq[\sum_{\kappa\kappa'}e^{i(\delta_\kappa+\delta_{\kappa'})}R(\mathrm{K},L,\mathrm{K}')\times$ang. mom. coupling coefficient] and then assembling the differential cross section through Fermi's golden rule No. 2. The main part of the program computes the radial matrix elements $R(\mathrm{K},L,\mathrm{K}')$ through a numerical integration which is a variation on the Runge-Kutta method. We give as an example the computation of $R_{\rm Coul}$ for an electric quadrupole transition ($L=2$) using seven partial waves. For each value of the integration variable x, the program computes the cutoff function C_1, which is an integrand $j_L(\epsilon x)h_L(\epsilon x)\rho_1(x)x^2$, and the Coulomb wave functions f and g which are the solutions to coupled first-order radial Dirac equations. In this example there are 72 values for f and g running over the quantum numbers $\pm\mathrm{K}$ and $\pm\mathrm{K}'$ for the incident and outgoing electron, respectively. With these values at x of $f_{\rm K}$, $f_{\rm K'}$, $g_{\rm K}$, $g_{\rm K'}$, and C_1 the integration is carried out up to that point. The program repeats these calculations of the Coulomb wave functions and cutoff functions over the nuclear Coulomb field from the center of the nucleus to an asymptotic region which for our energies is $\geq$20 000 F. The radial integrals are then normalized and the phase shifts for each K and K′ are computed. Finally, the cross section is assembled as outlined above.

The program yields a relative cross section which is defined as the ratio of the differential cross section to the reduced nuclear transition probability. The total cross section, which is the quantity of interest in our work, is calculated by summing the squares of the coefficients of the spherical harmonics. The program then computes the quantity $\sigma/(B/e^2)$, where B is the reduced transition probability.

B. Results

Tests of the model independence of the calculation presented in Table I show a small, 1–2%, change in total cross section for large, 10%, changes in nuclear half-density radius and skin thickness. Since the half-density radius is known to within 2% and skin thickness

to within 10%, further modification of these figures will not significantly change the result of the program in the energy range considered. Since the transition charge currents and magnetization densities, i.e., ρ_1, ρ_2, ρ_3, and ρ_4, in some instances change by factors of 3 for a 10% change in c, the half-density radius, and/or t, the skin thickness, the insensitivity of σ is taken as a demonstration of model independence and correct normalization of the program. Ziegler and Peterson[18] have investigated this question extensively, and we agree with their conclusion that the differences due to variations of c and t in the model used yield small differences in the cross section.

Tests of convergence of the cross section versus number of partial waves indicated that, in the energy region and for the transition multipolarities of interest in our study, seven partial waves were sufficient. Later modification of the output of our program allowed the contribution of each partial wave to be seen.

Typical computational results are shown in Fig. 2, in which the contributions from individual partial waves for inelastic scattering of electrons with incident energy T_0 from the 1.078-MeV state in ^{115}In are shown together with the total PWBA cross section for that state. Here the transition is taken to be $M1$. Since the program could also calculate the contributions from the individual partial waves for the PWBA, of interest are

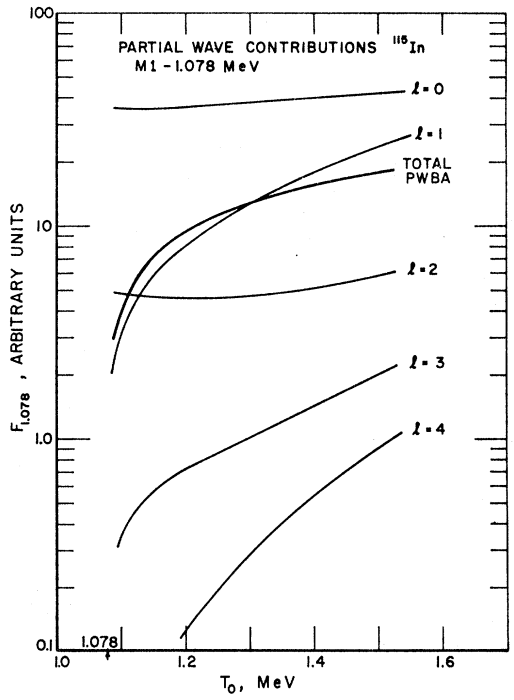

FIG. 2. Individual wave contributions are plotted as F_l, which is proportional to partial $\sigma_l/B(M1,\uparrow)$, versus incident electron kinetic energy. The F's are calculated in the DWBA by the Duke program for an $M1$ transition to the 1.078-MeV state in ^{115}In. For comparison the total PWBA for the same transition is given.

[18] J. Ziegler and G. Peterson, Phys. Rev. **165**, 1337 (1968).

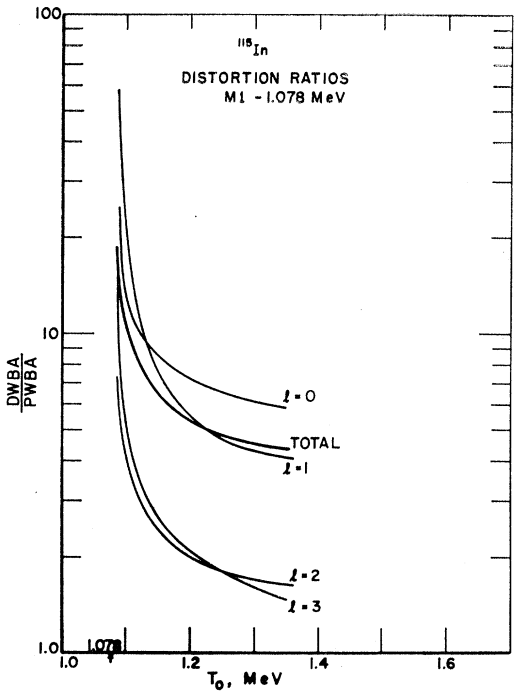

FIG. 3. The ratio of the DWBA to PWBA for the partial F_l's are plotted versus incident electron kinetic energy for a magnetic dipole transition to the 1.078-MeV level of ^{115}In. The same ratio is plotted for the total $F(M1)$.

the distortions of the individual waves when calculated by partial-wave analysis for the Coulomb potential compared to the plane-wave results. These data are plotted in Fig. 3 as ratios. Also included is the distortion of the total cross section.

The large contribution of the $l=0$ partial wave in Fig. 2 is expected for the $M1$ transition since the magnetic dipole results mainly from a spin-flip transition with little or no contribution from the relative orbital angular momentum components of the electron-nucleus interaction. The s wave, because there is no centrifugal repulsion, is most distorted since it spends the most time, relative to the other waves, within the nuclear surface. It is interesting to observe that the finite-tip effect at essentially threshold electron energy is due to the s-wave interaction.

Figures 4 and 5 are corresponding graphs for the $E2$ transition. For $L=2$, $l=2$, 1, and 3, in order of decreasing importance, is observed. Although the s and p waves are highly distorted, these contributions to the total cross section are small at low energies, $l=1$ becoming more significant at higher energies. As noted in the Introduction, previous attempts to patch up the PWBA by using the nuclear Coulomb function indicated distortion factors of 2–5.[5] From Fig. 3, the distortion factor for $M1$ excitation varies from about 10 at 25 keV above threshold to 4.5 at 200 keV above threshold. The comparable enhancements over PWBA for $E2$ excitations from Fig. 5 are 6 and 2.6.

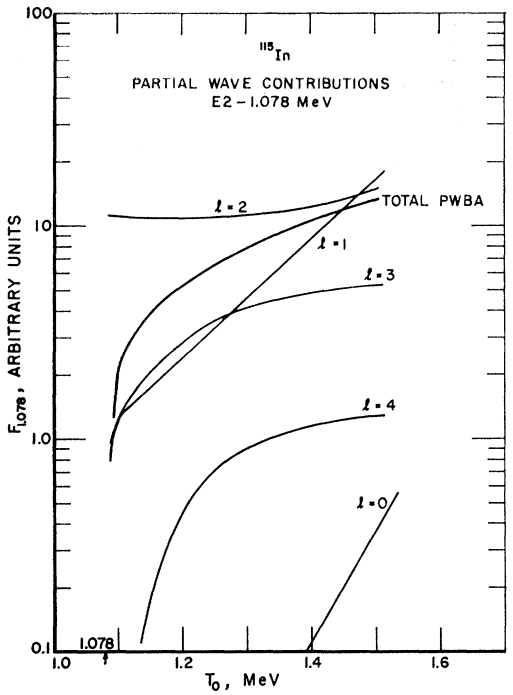

FIG. 4. Same parameters plotted as in Fig. 2 for an $E2$ transition.

Figure 6 shows the data for $M1$, $E2$, and $M3$ DWBA along with experimental electron excitation function for the 1.078-MeV level of ^{115}In. The PWBA is also shown for reference. These excitation functions include only the normalization form the Duke program. The

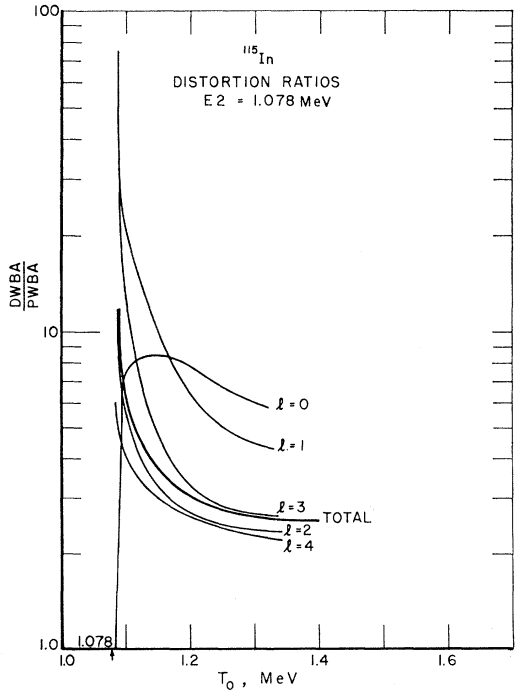

FIG. 5. Same ratios plotted as in Fig. 3 for an $E2$ transition.

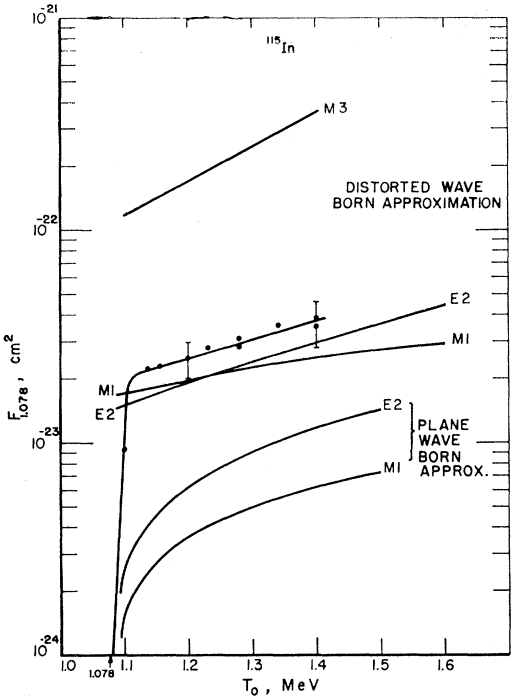

FIG. 6. The experimental excitation function for the 1.078-MeV state of ^{115}In [Eq. (12)] is compared to the theory which is expressed by the same electromagnetic parameter F through (4) and (5). The data are absolute, i.e., F_{th} is neither relative nor dependent on nuclear model. The experimental curve is subject to a shift of $\pm 35\%$ due to possible errors in $\Gamma_{\text{iso}}/\Gamma\int\sigma_\gamma dE$ and/or small contributions from the 1.133-MeV state. DWBA values of other F's at 1.3 MeV are 8.5($E1$), 75.3($M2$), and 83.8($E3$) in barns.

relatively good absolute agreement of the magnitude and slopes indicates the possibility of a mixture of $M1$ and $E2$ transitions. Equation (9) can be used to calculate a mixing ratio a if the crossing point of the $M1$ and $E2$ lines is transposed to the experimental line. We can see that this must be done when $F(E2) = F(M1)$ since at that excitation energy the value of $F_{\text{expt}} = F(E2) = F(M1)$ independent of a.

If we assume $a \geq 0$, a is single valued and this number can be calculated if the multipolarities in the mixture bracket the experimental results. If the theoretical F's in the mixture have equal value at one energy, this value can be shifted to the experimental value at that energy because of present uncertainties in both experiment and theory (compare, e.g., with internal conversion[16]). A range of a can be calculated which can then be compared to a mixing ratio obtained from other experiments such as will be done in Sec. 4 with the results of nuclear photon self-absorption and Coulomb excitation of the same excited states of ^{115}In.

From Fig. 6 we get $0.5 \leq a \leq 2$ from the $M1$-$E2$ curves when $a = \Gamma_0(E2)/\Gamma_0(M1)$. For the $E2$-$M3$ mixture without shifting the $E2$ curve relative to experiment, one gets $a = \Gamma_0(M3)/\Gamma_0(E2) \simeq 0.03$. However, the latter mixing ratio is not invariant compared to the best-fit experimental curve because of the steeper slope of F_{M3}. Pure

electric quadrupole excitation is not ruled out, but we cannot decide this because of the experimental errors.

The next step in ^{115}In, which was investigated by the same means, is at 1.450 MeV. The excitation function was obtained by stripping the 1.078-MeV excitation function to about 2.0 MeV. These data are compared with the Duke program calculations. Since the slope of the $M1$ excitation function follows closely the slope of the experimental data and the magnitudes agree within 20%, the transition appears to be pure $M1$. The mixture with $E2$ is not possible unless $E2$ also has the same slope.

4. DISCUSSION

A. 1.078- and 1.450-MeV States of ^{115}In

From the comparison of experiments and the DWBA calculations in Sec. 3, both the 1.078- and 1.450-MeV states are $\frac{7}{2}^+$, where the lower state probably has considerable $M1/E2$ mixing while the 1.450-MeV state is essentially pure $M1$. Since separate measurements of Γ_0 and $\Gamma_0(E2)$ for the ground-state transitions have been made for these states by nuclear photon self-absorption and by Coulomb excitation, the mixing ratios measured in this way are quantitatively compared in Table II with those deduced from electron scattering in Sec. 3. The agreement confirms our analysis based on fitting F_{expt} versus T_0 with the Duke cross sections.

Independent of the electron-scattering measurements, the spin-parity of $\frac{7}{2}^+$ for the 1.450-MeV states comes from:

(a) the identification of the ground-state transition being $M1$ from our self-absorption measurements,[5,7] where $g\Gamma_0=1.7\pm0.6\times10^{-3}$ eV with a hindrance of 32 compared to the Weisskopf limit;

(b) the observation of isomer activation (as in Figs. 1 and 7) which indicates the spin is intermediate between $I_0=\frac{9}{2}^+$ and $I_{\text{iso}}=\frac{1}{2}^-$ where one expects the 1.450 MeV to cascade first to the $\frac{3}{2}^+$ 829-keV level[10];

(c) the upper limit from Coulomb excitation $B(E2,\uparrow)\leq80\ e^2\ \text{F}^4$ [12]; and

(d) the observation of the γ ray following β^- of $\frac{11}{2}^-$ ^{115m}Cd.[10] From the nuclear self-absorption and Coulomb-excitation measurements, the mixing ratio $a\leq0.32$ agrees with the pure $M1$ assignment from electron scattering.

TABLE II. Mixing ratios from photon absorption and Coulomb excitation compared to electron scattering.

Level in ^{115}In	$g\Gamma_0$ (eV) [a]	$B(E2,\uparrow)$ [b]	a [c]	a (electron scattering)
1.078 MeV	$2.8\pm0.8\times10^{-4}$ [d]	96 ± 18 [e]	0.7 ± 0.3	$0.5\leq a\leq2$
1.450	$1.7\pm0.6\times10^{-3}$ [d]	≤80 [e]	≤0.32	pure $M1$

[a] Assumes $\frac{7}{2}^+$ for each level, i.e., $g=0.8$.
[b] Units $e^2\text{F}^4$.
[c] $a=\Gamma_0(E2)/\Gamma_0(M1)$ for ground-state transition.
[d] References 5 and 7.
[e] Reference 12.

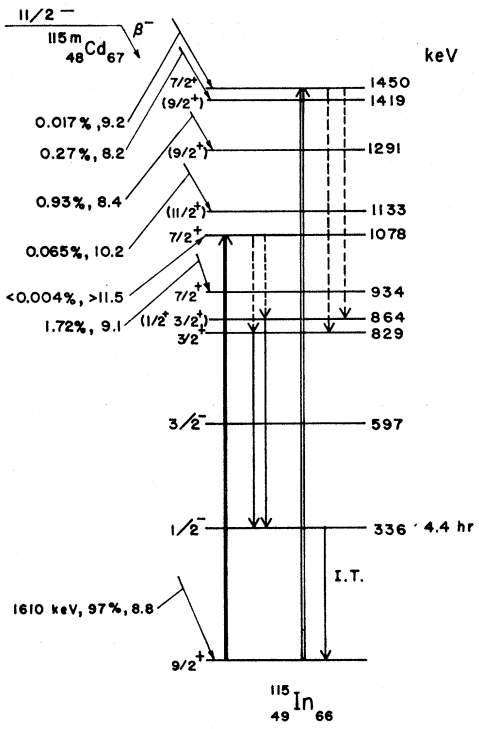

FIG. 7. The energy-level diagram of $_{49}{}^{115}\text{In}_{66}$ is presented up to 1.450 MeV. The two states excited by electroexcitation which cascade down to the 4.4-h isomer are shown as are our limits for the absence of β^- decay from ^{115m}Cd to the 1.078-MeV state of ^{115}In. The spin-parity assignments are taken from the work of Graeffe *et al.* with the exception of the assignments for 0.829-, 0.864-, and 1.078-MeV states.

Clearly, the 1.450-MeV state is not the $\frac{15}{2}^+$ member of a $K=\frac{1}{2}$ rotational band based on the 864-keV level as suggested in the work by McDonald *et al.*[12]

The support for the $\frac{7}{2}^+$ assignment to the 1.078-MeV parallels that for the 1.450-MeV level with one big exception. The absence of the 1.078-MeV γ ray from the β^- ^{115m}Cd provided the justification for our earlier assignment[5] of $\frac{5}{2}^+$ to the 1.078-MeV level. The β^- decay would then be third-forbidden and therefore retarded by $\sim10^5$ compared to the first-forbidden β^- transitions from $h_{11/2}{}^-$ ^{115m}Cd to the 0.934-, 1.131-, 1.291-, 1.419-, and 1.450-MeV states of ^{115}In where the logft values vary from 8.2 to 10.2. This information is summarized in Fig. 7. Nevertheless, two independent measurements of the ground-state radiative width of the 1.078-MeV level by the photon self-absorption method[5,19] together with two independent measurements of Coulomb excitation[12,20] are in agreement and predict large $M1/E2$ mixing, $a=0.7\pm0.3$, where $a=\Gamma_0(E2)/\Gamma_0(M1)$, in consonance with our electron excitation measurements as in Fig. 6 where we obtain $0.5\leq a\leq2$, but in

[19] Y. Cauchois, Y. Heno, and B. Boivin, Compt. Rend. **259**, 3233 (1964).
[20] D. Alkhazov, K. Erokhina, and I. Lemberg, Izv. Akad. Nauk SSSR, Ser. Fiz. **28**, 1667 (1964); Bull. Acad. Sci. USSR, Phys. Ser. **28**, 1559 (1965).

TABLE III. Photopeak-to-Compton edge ratios.

γ-ray spectrometer	Peak-to-edge ratios[a]
NaI(Tl) 6.3 cm diam×6.3 cm [b]	0.4:1
Ge(Li) 1.2 cc [c]	0.3:1
Ge(Li) 10 cc	0.6:1
Ge(Li) Duode −18 cc [d]	2:1

[a] Ratio in the 1.133-MeV photopeak compared to the Compton edge in the region of 1.078 MeV in the γ spectrum of ^{115m}Cd.
[b] Reference 23.
[c] Reference 10.
[d] Reference 24.

complete disagreement if the spin-parity were $\frac{5}{2}^+$ where the $E2/M3$ mixing is $\simeq$30 from the electron excitation function while it is $\simeq$0.7 from the radiative width measurements.

The $\Gamma_0(M3)/\Gamma_0(E2)$ mixing ratio, in addition to disagreeing with our electron-scattering measurements, predicts a large Γ_{M3} enhanced, by $\sim 10^8$, over the Weisskopf limit, and it is at complete variance with systematics on radiative widths.[21] Measurement of radiative widths of ^{115}In in progress,[22] using nuclear resonance fluorescence, appear to verify the predominant $M1$ character of the 1.078-MeV state and states in the 1.45-MeV region of ^{115}In when interpreted in light of recent Coulomb-excitation results.[12]

B. Search for ^{115m}Cd $\xrightarrow{\beta^-}$ ^{115}In, 1.078-MeV Level

In view of the importance of this energy level in establishing a well-understood test case for comparison of experiment and theory in threshold-energy electron excitation, a search for the 1.078-MeV γ ray following β^- of ^{115m}Cd was first made with a 10-cc Ge(Li) detector and then with a Duode Ge(Li) pro-Compton spectrometer. Earlier measurements of the γ-ray spectrum with NaI(Tl) crystals[23] and a 1.2-cc Ge(Li) detector[10] had large Compton edges in the 1.10-MeV region from the 1291-keV γ ray which would have obscured any evidence for a weak 1078-keV line. Comparisons of the sensitivity, i.e., photopeak-to-Compton edge ratio, are given in Table III.

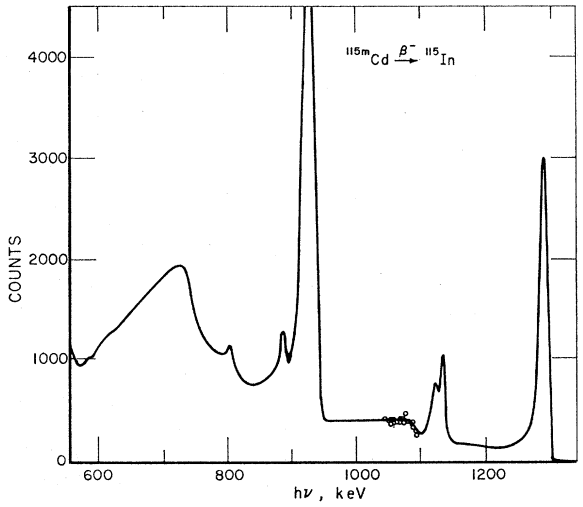

FIG. 8. The spectrum of γ rays in the 600–1300-keV region following β^- decay of ^{115m}Cd is presented. An 18-cc Ge(Li) Duode spectrometer was used and peaks are seen at 1291, 1133, 1120, 934, 888, and 805 keV. The lines at 1121 and 888 keV come from a ^{46}Sc impurity in the ^{115m}Cd source and the 805-keV line is of unknown origin. The favorable Compton reduction in the 1078-keV region allows one to set a 500:1 lower limit on the 934- to 1078-keV γ-intensity ratio.

A short description of the measurement follows. A 30-μC 43-day ^{115m}Cd solution with the ^{110m}Ag removed by precipitation with AgCl was obtained from a commercial supplier. However, measurements with the 10-cc Ge(Li) revealed trace amounts of ^{46}Sc with γ lines at 888 and 1121 keV. Evidence for the 1078-keV γ ray was negative and with the improved Compton edge reduction, a lower limit of 35:1 for 1133- to 1078-keV γ rays was established. Next, to further suppress the Compton distribution in the region of interest, the γ spectrum was measured by a Duode γ-ray spectrometer.[24] The Duode consists of two Ge(Li) diode detectors within a single crystal of germanium where each detector is approximately 9 cc and the pair are run in coincidence. When Compton events occur in both diodes, the outputs are summed and counted, i.e., full energy events are rejected from either diode detector. The ^{115m}Cd $\xrightarrow{\beta^-}$ ^{115}In γ-ray spectrum for an 18-h run in the 600- to 1300-keV region is presented in Fig. 8. The Compton-like edge at 725 keV appears to result from the 485 feeding the 934. This most probably obscures the cascade from the 1450- to 864- and/or 829-keV states which is presumably the primary mechanism in feeding the 4.4-h isomer at 336 keV. With the greatly suppressed Compton edge and tail in the region of interest, no evidence for the 1.078-MeV γ ray is seen. The lower limit of the 1.133- to 1.078-MeV γ's is approximately 20:1 and the limit of 0.934- to 1.078-MeV γ rays is greater than 500:1. From this result we can infer a $\log ft > 11.5$ for the β^- transition to the 1.078-MeV level compared with a value of 9.1 to the $\frac{7}{2}^+$ 0.934-MeV state. These limits are included in Fig. 7.

It appears that the absence of a β^--decay transition to the 1.078-MeV level constitutes a presently rare example of large retardation in first-forbidden unique β^- transitions induced by phonon rather than single-particle mixing between the $h_{11/2}^-$ neutron and $\frac{7}{2}^+$ 1.078-MeV final state in ^{115}In. Other examples of phonon-hindered transitions have been observed in Rh, Sb, and I.[25]

[21] N. Gove, in *Nuclear-Spin Parity Assignments* (Academic Press Inc., New York, 1966).
[22] W. Alston (private communication).
[23] J. van der Kooi, H. van den Bold, and P. Endt, Physica **29**, 140 (1963).
[24] A. Sayres and J. Baicker, IEEE Trans. Nucl. Sci. **NS-15**, No. 3 (1968).
[25] W. Walters (private communication); Massachusetts Institute of Technology, Laboratory of Nuclear Science Report No. 905-81, 1966 (unpublished).

C. Status of ^{115}In

The spectrum of ^{115}In has been studied extensively in the β^- decay of ^{115m}Cd and ^{115g}Cd, excitation studies of ^{115}In with $^{14}N^{+5}$, $^{4}He^{++}$, and $^{16}O^{++}$, electron scattering and photoabsorption. Figure 7 is an energy-level diagram of ^{115}In up to 1.450 MeV. Earlier studies indicated that the spectrum of states between 1 and 1.5 MeV resulted from j-j coupling of the $g_{9/2}$ hole in the photon shell with a 2^+ core vibrational phonon from $_{50}{}^{116}$Sn, i.e., weak-coupling model, since all the even-parity states with angular momentum $|2-\frac{9}{2}| \leq J \leq 2+\frac{9}{2}$ had been tentatively identified in ^{115}In. Further, the center-of-gravity rule applied to the energies of the five states gave the approximate energy, 1.27 MeV, of the 2^+ collective state of ^{116}Sn, and the strength of this vibrational state of ^{116}Sn, $B(E2,\uparrow) = 2120\ e^2\ \mathrm{F}^4$ agreed with the sum of the $B(E2,\uparrow)$ of the five states of ^{115}In.[12] Recent measurements of internal-conversion electrons in $^{115g}\mathrm{Cd} \xrightarrow{\beta^-} {}^{115}\mathrm{In}$ by Bäcklin *et al.*[11] identified a rotational band in ^{115}In based on the $\frac{1}{2}^+$ state at 864 keV and confirmed the studies of Graeffe *et al.*[10] which discovered the main γ-ray cascade which populates the 336-keV $(\frac{1}{2}^-)$ isomer of ^{115}In. The cascade to the isomer from higher levels is of interest since we measure the product $B(L,\uparrow)\times\Gamma_{\mathrm{iso}}/\Gamma$ for both electron and photon excitation. For the product to be measurable, the level of interest has to be coupled fairly strongly to the ground state and an intermediate excited state, which, in the case of 1.078- and 1.450-MeV states, is not the isomer directly but the 829 $\frac{3}{2}^+$ level. It may be that isomer-activation measurements mainly pick out states with strong interband mixing. McDonald[12] has recently examined the 1–1.5-MeV region of ^{115}In with Coulomb excitation, β^--γ, and γ-γ coincidences from ^{115m}Cd. They show that the j-j coupling model disagrees in detail with as many data as it explains, and that the rotational band built on the 864-keV level predicts two incorrect energies in the 1–1.5-MeV region and, as we have shown, two incorrect angular momenta, $\frac{5}{2}^+$ for the 1.078- and $\frac{15}{2}^+$ for the 1.450-MeV states.

It appears that neither approach fully explains the six positive-parity states between 934 and 1450 keV. One could extend the j-j coupling model by coupling the $p_{1/2}{}^-$ single-particle state to an octupole vibration. Both are collective phenomena in this mass region where the octupole vibrations in ^{116}Sn, ^{120}Sn, and ^{124}Sn have been recently measured by electron scattering[26] and well described in terms of the microscopic quasiparticle second Tamm-Dancoff theory.[27] Another approach would be to explore the positive-parity states through interactions of the spherical states ($g_{9/2}{}^+$ and $p_{1/2}{}^-$) with the two positive-parity deformed levels at 829 and 864 keV which appear to form a $K=\frac{1}{2}$ rotational band.

5. CONCLUSIONS

Comparison of electron excitation of nuclear levels in ^{115}In with the Duke inelastic-electron-scattering program show that spin and parity assignments can be made to the levels and mixing ratios can be assigned to the transitions in agreement with assignments from lifetime and Coulomb-excitation measurements. Thus the 1.078- and 1.450-MeV states of ^{115}In are both $\frac{7}{2}^+$ with $M1/E2$ mixing ratios, $a=0.7\pm0.3$ and ≤ 0.3, respectively, where $a=\Gamma_0(E2)/\Gamma_0(M1)$. The Duke DWBA calculation provides a major step in obtaining quantitative spectroscopic data from threshold-energy electron scattering. We have attempted to show in detail how one makes the comparison between experiment and theory using other measurements of the same transitions to corroborate this comparison.

The number of nuclei studied by the electron and photon activation method is growing,[7,28,29] i.e., ^{87}Sr, ^{111}Cd, ^{113}In, ^{117}Sn, ^{137}Ba, ^{179}Hf, ^{195}Pt, and ^{199}Hg, and, dependent on the accuracy of the bremsstrahlung flux, mixing-ratio assignments within a factor of 2 should be possible using the methods outlined in this paper. Since the method selects $M1$ and $E2$ transitions, the collectivity of the transitions can be specified. Although not observed to date, electric monopole transitions of $\Gamma_{e^\pm} \gtrsim 10^{-8}$ eV should be visible by this method since $\sigma_{\mathrm{iso},e} \simeq 10^{-35}$ cm^2 are measurable. The natural selection of nuclear states with sizable interband mixing as in the spheroidal and rotational structures of ^{115}In will become clearer after more comparisons between experiment and theory are made, together with more data from measurements of Coulomb excitation of odd-A nuclei.

ACKNOWLEDGMENTS

The authors wish to thank Dr. J. W. Motz for the hospitality and support extended to us at the National Bureau of Standards. The calculations were done at the NBS Computation Center. We are indebted to Dr. L. C. Biedenharn and Dr. E. Guth for early interest in the theoretical problem. The remarkable patience and efforts of Dr. D. S. Onley and Dr. S. T. Tuan in helping us interpret and use their Duke inelastic-electron-scattering program at threshold energies is greatly appreciated. One of us (B.T.C.) wishes to acknowledge the hospitality and help in the Ge(Li) Duode measurements of Dr. J. Baicker and Dr. A. Sayres of Princeton Gamma Tech. Discussions on the manuscript with Dr. D. Dreschel and Dr. C. E. Dick have been most helpful.

[26] P. Barreau and J. Bellicard, Phys. Rev. Letters **19**, 1444 (1967).

[27] A. Rimini, J. Sawicki, and T. Weber, Phys. Rev. Letters **20**, 676 (1968).

[28] C. Dick, B. Chertok, and W. Johnson, Bull. Am. Phys. Soc. **12**, 596 (1967).

[29] E. Booth and J. Brownson, Bull. Am. Phys. Soc. **13**, 718 (1968).

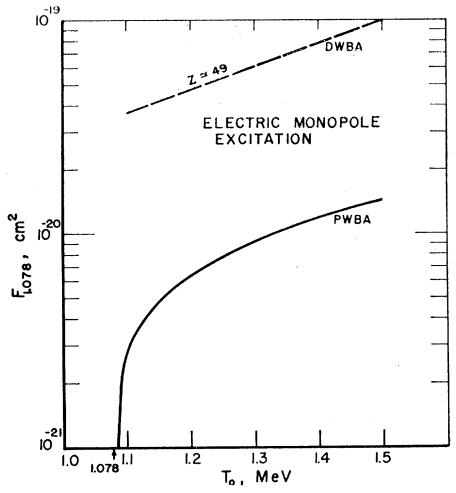

FIG. 9. F_{C0} is plotted versus electron kinetic energy for a 1.078-MeV electric monopole transition, $I_i^\pi = I_f^\pi$, in ^{115}In. The DWBA curve comes from the calculation of Ter-Martirosyan. The similarity in magnitude of the distortion with F_{E2} in Fig. 6 is expected.

APPENDIX

We present an explicit calculation of the integrated inelastic-electron-scattering cross section in the long-wavelength limit, $q \to k$, for electric monopole excitation where $I_i^\pi = I_f^\pi$. Ter-Martirosyan has derived the threshold $E0$ cross section in the DWBA,[30] and we shall use one of his results in Fig. 9.

The starting point in the calculation is the instantaneous Coulomb interaction cross section in the PWBA,

$$\frac{d\sigma}{d\Omega}(CL) = \frac{4\pi\alpha^2}{[(2L+1)!!]^2}\frac{q^{2L}}{{p_0}^2}B(CL,q,I_fI_i)V_L(\theta),$$

which for $L=0$ becomes

$$\frac{d\sigma}{d\Omega}(C0) = \frac{4\pi\alpha^2}{{p_0}^2}B(C0,q,I_fI_i)V_L(\theta),$$

where the reduced nuclear transition probability

$$B(C0,q,I_fI_i) = (q^4/144\pi)\left|\langle\Psi_N{}^f|\int r^2\rho(r)d^3r|\Psi_N{}^i\rangle\right|^2$$
$$= \frac{q^4}{144\pi}\frac{135\pi}{\alpha^2\hbar c}\frac{\Gamma_{e^\pm}}{k^5}.$$

$\Gamma_{e^\pm}$ is the width of the excited state in ground-state transitions involving internal conversion, internal pair creation, two-photon emission, etc. Writing out the longitudinal kinematic factor $V_L(\theta)$, the differential cross section becomes

$$d\sigma_{C0} = \frac{4\pi 135}{144\hbar c}\frac{\Gamma_{e^\pm}}{k^5}\frac{1}{{p_0}^2}\int p_0p(2{p_0}^2+2p^2+4-q^2-k^2)d\Omega.$$

It is convenient to integrate over q, i.e., $p_0pd\Omega = 2qdq$, and then

$$\sigma_{C0} = \frac{30\pi}{\hbar c}\frac{\Gamma_{e^\pm}}{k^5}\frac{1}{{p_0}^2}[({p_0}^2+p^2+2-\tfrac{1}{2}k^2)p_0p-(p_0p)^2].$$

Putting the result in the form of (5), $\sigma_{C0} = F_{C0}\Gamma_{e^\pm}/m_0c^2$, one obtains

$$F_{C0} = \frac{30\pi}{\lambda}\frac{1}{k^5}\frac{1}{{p_0}^2}[({p_0}^2+p^2+2-\tfrac{1}{2}k^2)p_0p-(p_0p)^2].$$

The expression in brackets differs from Ter-Martirosyan's cross section (for $\alpha Z \to 0$) by $\frac{1}{2}(p_0-p)^2$ and the multiplicative factors are different since we have used the reduced form of B and the explicit transition width $\Gamma_{e^\pm}$.

In Fig. 9, F_{C0} versus T_0 is plotted for the 1.078-MeV excitation. A factor comparable to F has been plotted by Ter-Martirosyan for $k=1$ MeV, $Z=50$, for DWBA and PWBA. We have used his enhancement factors to correct our F_{C0} since Tuan *et al.*[6] do not calculate the monopole cross section in their partial-wave analysis program. The distortion factors of about 7× at threshold are what one would expect since there is more distortion in $E0$ than $E2$ transitions because the former cross section is only finite for penetration of the electron waves inside the nucleus. It is here that the Coulomb distortion effects should be greatest.

[30] K. Ter-Martirosyan, Zh. Eksperim. i Teor. Fiz. **20**, 925 (1950).